

Title: Earth/Moon System Star Tracking Sensor for Improved Deep Space Laser Communications

Stephen Cain, Air Force Institute of Technology

Michael Licher, NASA Glenn Research Center

Abstract:

The goal of this research is to improve deep space communication links by exploring a new concept in stellar navigation that uses images of the Earth/Moon system to obtain precise pointing information so that the laser signal from the satellite can be directed at the ground station with unprecedented accuracy. Currently, the concept for satellite pointing relies on a dual axis star tracker that compares images of the celestial sphere to a star catalog to obtain a 3-axis orientation solution. Most star trackers are designed with a wide field of view (required to obtain enough bright stars to achieve a navigational fix) and only provide reliable pitch and yaw estimates thus necessitating the use of a second star tracker looking at an axis perpendicular to the first one to obtain an accurate estimate of the roll of the spacecraft.

In the new concept the optical design will be modified to ensure that both the Earth and the Moon will be within a narrow field of view centered on Earth relative to the field of view of most star tracking systems. Because of the proximity of the bodies, it is possible to obtain highly accurate estimates of the pitch, yaw and roll of the spacecraft relative to the Earth/Moon system. The new tracker will allow for accurate 3-axis control of the spacecraft from a single tracker thus allowing the second star tracker, which would normally be pointed in a direction perpendicular to the one pointed at earth, to obtain the spacecraft roll estimate. This wide field star tracker facilitates functions like the initial satellite pointing during the acquisition phase of establishing the laser communication link or solving the lost in space problem should the system need to be reset. This new design will be tested in simulation and compared for 3-axis pointing accuracy against a standard commercial star tracker.

1. Introduction:

Many advanced satellites require accurate and precise orientation towards the Earth. This applies to remote sensing, communications, space exploration, and weather satellites to name a few. In order for the satellite to be oriented properly, knowledge of the current orientation must first be determined relative to the celestial sphere. Star tracking systems provide the highest degree of accuracy over long periods of time, compared to other attitude sensors, because the star positions in the celestial sphere do not significantly move over time. Additionally, the star tracking system orients to multiple objects with very small angular extents yielding less error [1].

Determining the attitude of a satellite from a star-tracker normally requires an observation from an imaging system that employs an object detection method and a star map containing a catalog of known star positions [1,2]. The attitude of the satellite with respect to the celestial

reference frame is given by the angular change between orientation of the star map and the observations from the imaging system. A significant difficulty in star-tracking is the ability to observe a large enough part of the sky to ensure that there will be a sufficient number of stars to track. This design objective competes with the desire to obtain a high degree of angular accuracy per pixel in the detector array collecting the star images. These competing objectives leads to star tracker designs that provide insufficient accuracy for laser communication systems.

The problem of star tracking to provide laser communications from deep space probes and Earth; however, does not need to suffer the same design challenges that a normal star tracker must overcome. Because the satellite must point a sensor at the Earth to establish and maintain a communication link, thus the need to obtain sufficient stars in the field of view of the star tracker is reduced, since a known source must be present in the desired field of view. The idea of tracking the Earth itself is not new and has been investigated previously [3]. Problems arise from the fact that the Earth is illuminated in a non-uniform manner depending on the angle of observation relative to the angle from which the Earth receives its sunlight. This leads to ambiguity on the location of the centroid of the Earth at any given time.

In order to mitigate the effect of the illumination phase of the Earth as viewed by the star tracker, we will use the fact that the star tracking sensor is also viewing the Moon at the same time it is viewing the Earth. The Moon will be illuminated by the sun in the same way the Earth is as perceived from a spacecraft out at the orbit of Mars or beyond. Figure 1 shows the sensing concept for the new star tracker. The Earth will typically occupy a small number of pixels, thus making estimates of the exact location of the planet susceptible to error from noise, illumination and albedo variation that corrupt the estimate of its centroid. The angle between the partially illuminated Earth and Moon will be used to estimate the spacecraft roll, thus reducing the uncertainty in the Earth's position relative to the stars due to illumination phase, since the moon will be in the same phase as the Earth.

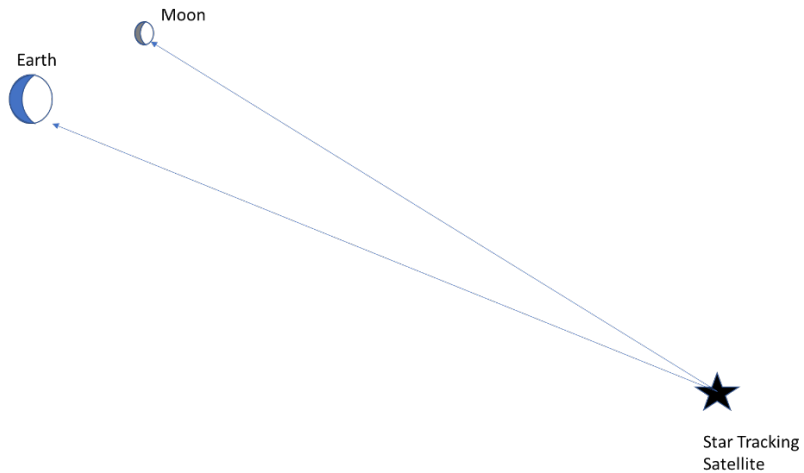


Figure 1: Earth/Moon Star Tracker Concept

The remainder of this paper is organized as follows: Section 2 will introduce the basic star tracker imaging and data processing model. This will include specifics of a commercial off the shelf star tracker that could be used for the intended application of finding and tracking the Earth's location. Section 3 introduces the design of the new Earth/Moon star tracker as well as its associated data processing chain. Section 4 contains results obtained from processing the simulated data sets introduced in the previous sections and Section 5 contains a discussion of conclusions drawn from the research.

2. Commercial Star Tracker Model

The research makes use of a model of a star tracker model based on one that is in use today. Of the many possibilities, the Space Micro uStar-x00M series rad hard system with quaternion and rate output is chosen as representative technology today to help establish the different parameters of our star tracker system so as to give practical results. The focal plane sensor itself, made by On Semiconductor, is a HAS2 High Accuracy CMOS Active Pixel Image Sensor. The specifications used in simulations for this research of this star tracker are shown in Table 1.

Table 1: Commercial off the shelf star tracker specifications

Item	Value	Units
Aperture	50	mm
F#	1.8	f/D (unit-less)
CCD	1024X1024	pixels
Pixel Pitch	18	um
Lens	Rad-Hard Glass	N/A
Output	Quaternion and Rate	Quaternion Vector

Pristine images of the Earth as seen from Mars (without the sensor model effects) are simulated using Starry Night digital planetarium software. Figure 2 shows a labeled image of the Earth from the vicinity of Mars orbit predicted for the date of June 14, 2025.



Figure 2: Pristine image of the Earth and Moon from Starry Night™ as seen from Mars on June 14, 2025

The reflectivity of the Earth was scaled so the min to max values ranged between 0 and 0.75 (to represent bright clouds). The moon albedo was scaled to range between values of 0 to 0.25 as its surface has more consistent reflectivity. This image will also appear in the focal plane of the star tracking camera as the image predicted by geometric optics if the detectors are 1/200 the size of the star tracker's pixels. This is because the sampling of the source image is chosen to correspond to 1 microradian per pixel.

Next, a radiometry model was used to compute the number of photons coming from each pixel in the source image received by the star tracking camera using the albedo, r , as discussed previously with specifications found in Table 1. Equation (1) shows how the number of photons, Q , arriving in each pixel of the pristine image is computed. The Earth and Moon are assumed to be illuminated by light from the sun with an intensity of 1000 watts per square meter across the entire visible band [4].

$$Q = \frac{1000qrTA\pi D^2\lambda}{hc\pi z^2} \quad (1)$$

In this equation q is the quantum efficiency of the typical photodetector in the star tracker array. T is the integration time of the detector (about 0.1 seconds for a 10hz frame rate). A is the area of each pixel in the source array ($6.5e10$ square meters). D is the diameter of the receiver optic, h is Plank's constant, c is the speed of light in a vacuum, z is the distance from Mars to the Earth (about 1.6 AU at the time simulated) and λ is the center wavelength of the light admitted by the detector array (around 500 nanometers).

The imaging system model assumes that the points on the Earth and Moon that reflect light from the sun will produce plane waves at the distant receiving aperture of the star tracker. To calculate or predict what the field will be in a distant plane given a field in a source plane, the Rayleigh-Sommerfeld diffraction equation can be used. With a source plane of area extent of Σ and a field given by the phasor U_s , the field produced in a distant plane is given by Equation (2) [4].

$$U_r(x, y) = \frac{z}{j\lambda} \iint_{\Sigma} \frac{U_s(\xi, \eta)}{r_{12}^2} \exp\left(\frac{j2\pi r_{12}}{\lambda}\right) d\xi d\eta, \quad (2)$$

where r_{12} is the distance between the points under consideration in each plane. Here the variables of integration over the area are η and ζ . The distance r_{12} is found as:

$$r_{12} = \sqrt{z^2 + (x - \xi)^2 + (y - \eta)^2} \quad (3)$$

In this case the point spread function (PSF), h , for the optical system described in Table 1 is computed by taking the squared magnitude of the received field U_r . The PSF of this system is shown in Figure 3 on the same grid as the image of the Earth and Moon shown in Figure 2.

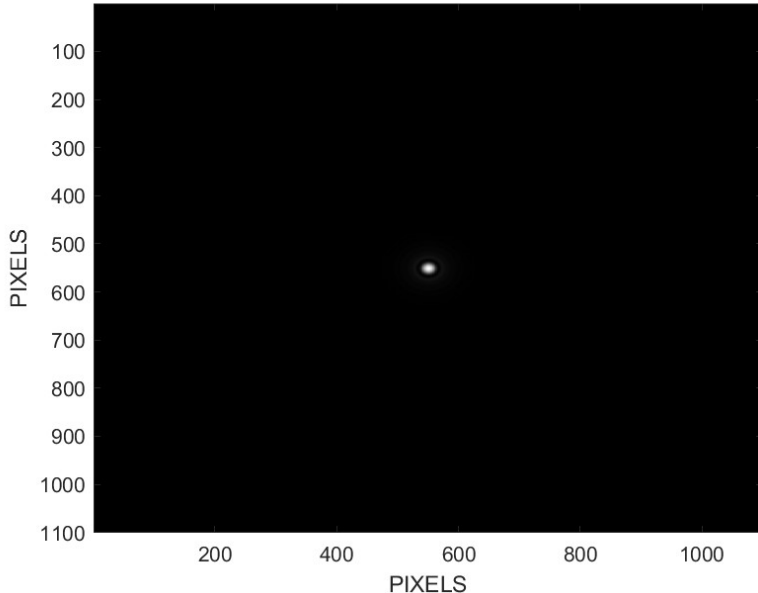


Figure 3: PSF of commercial star tracking camera

Assuming that the system is linear in intensity, the image of the Earth/Moon system formed on the detector array is the convolution of the image shown in Figure 2, $o(x,y)$, with the PSF of the camera system shown in Figure 3.

$$I(x_d, y_d) = \int_{-\infty}^{\infty} \int_{-\infty}^{\infty} o(x, y) h(x_d - x, y_d - y) dx dy \quad (4)$$

In this equation (x_d, y_d) are coordinates in the plane of the detector array in the star tracker. The image $o(x, y)$ is the image predicted by geometric optics shown in Figure 2, magnified to by the optical system. It is still sampled in angle space by the same 1 mrad sampling. The angular extent of the detectors in the star tracker are equal to 200 mrad. This is calculated by taking the 18 μm pixel size reported in Table 1 and dividing it by the 90 mm focal length of the star tracker optics. In order to produce the sampled image output by the detector array, $I(x_d, y_d)$ is convolved with a rectangle that is 200 samples on a side and then the output of that convolution is sampled every 200 samples horizontally and vertically. Figure 4 shows an image of the Earth as viewed by the commercial star tracker.

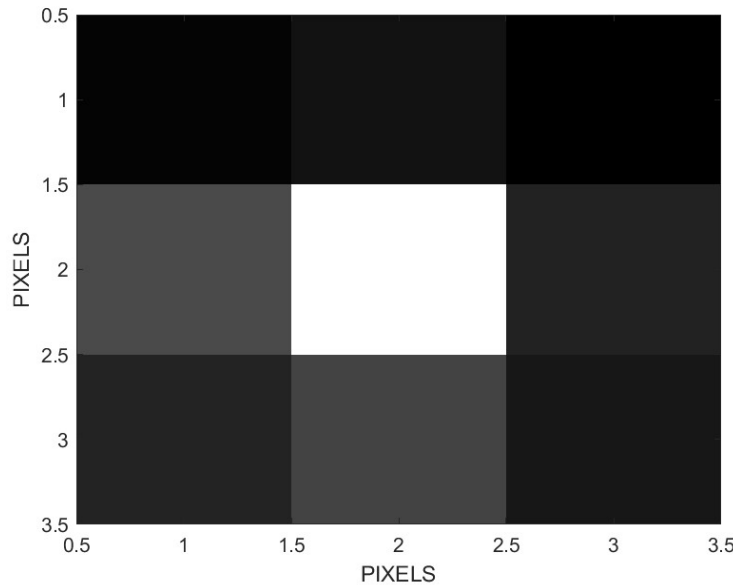


Figure 4: Earth as seen by the commercial star tracker

To this image Poisson noise is added by using the mean number of photons available in each pixel in Figure 4. Readout noise is also added to the image by generating a Gaussian random number at each pixel with a mean of zero and a standard deviation of 8. This number is added to the Poisson random number to produce the detector output.

The location of the Earth on the detector array is computed via a centroiding operation. Using threshold detection results, the bright Earth becomes the center of a region of interest (ROI) is defined as window of pixels surrounding the Earth. The centroid, or sometimes called the weighted sum technique, of the star is then calculated by the following equations:

$$\kappa_x = \sum_{x=R_s+1}^{R_e-1} \sum_{y=R_s+1}^{R_e-1} \frac{x \cdot d(x, y)}{B_{ROI}}$$

$$\kappa_y = \sum_{x=R_s+1}^{R_e-1} \sum_{y=R_s+1}^{R_e-1} \frac{y \cdot d(x, y)}{B_{ROI}}$$

Where the BROI is the total number of photons in the entire ROI, Rs and Re are the ROI start and end respectively, the κ_x and κ_y are the centroid values of the x and y locations on the array, the $d(x, y)$ is the number of photons at the pixel located at the coordinates x and y [4].

3. Earth/Moon Tracker

The proposed star tracker is not designed to navigate using stars but is specifically designed to aid in the pointing of a spacecraft at the Earth. In order to accomplish this, the optical and detector design is changed to achieve improved spatial resolution over the previous star tracker at the expense of the field of view. In this way, the new sensor cannot realistically find itself, if lost in space but can find the Earth and point at a specific location on the Earth if the Earth is in its field of view. For this reason, it must be paired with a commercial star tracker to be able to accomplish the mission of pointing the spacecraft at the Earth. The commercial star tracker points the spacecraft in the general vicinity of the Earth and the Earth/Moon tracker refines the pointing to a specific place on the Earth.

This would seem to suggest that two-star trackers are needed where only one might be utilized, however, a spacecraft will typically be equipped with two-star trackers. This is due to the fact that a single star tracker can estimate the pitch and yaw of the spacecraft but not the roll. In most cases a second star tracker is utilized that is looking in an orthogonal direction to the first star tracker so the roll can be estimated accurately. In the new configuration, proposed in this paper, the two-star trackers would be co-aligned. The first would be the wide field of view star tracker which can get the spacecraft pointed roughly in the vicinity of the Earth/Moon system and the second star tracker will be the narrow field of view sensor that can refine the pitch and yaw estimates and provide a suitable estimate of the spacecraft's roll.

The specifications for the Earth/Moon tracker are shown in Table 2. The CCD array is similar to the Allied Vision Stingray 504-B, which is a commercially available design that is not currently qualified for space.

Table 2: Earth/Moon Tracker Specification

Item	Value	Units
Aperture	50	mm
F#	8	f/D (unit-less)
CCD	2452 X 2056	pixels
Pixel Pitch	4.0	um
Lens	Rad-Hard Glass	N/A
Output	Quaternion and Rate	Quaternion Vector

The point spread function for this star tracker is computed in the same way the PSF was computed for the commercial star tracker, resulting in the image shown in Figure 5.

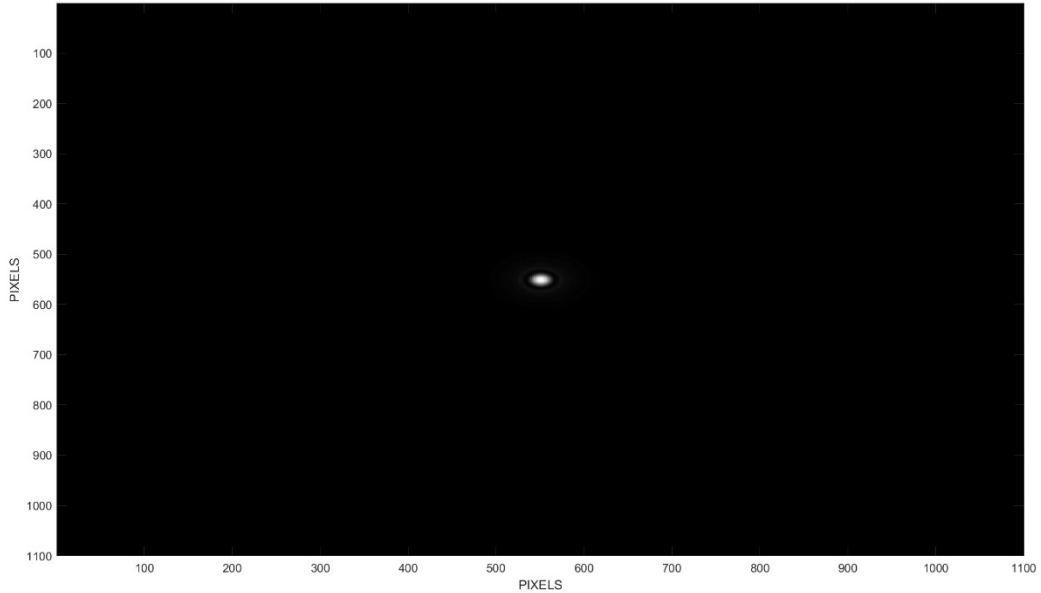


Figure 5: Earth/Moon tracker PSF simulated using data from Table 2.

The PSF is convolved with the pristine image of the Earth/Moon system and then convolved with a square that is 10 pixels on a side. This represents the effect of spatial integration on the detector surface which is 10 microradians in angle space (4 micrometer detector divided by .4-meter focal length). Poisson and readout noise are added in the same way as before to produce the image shown in Figure 6 of the Earth/Moon system

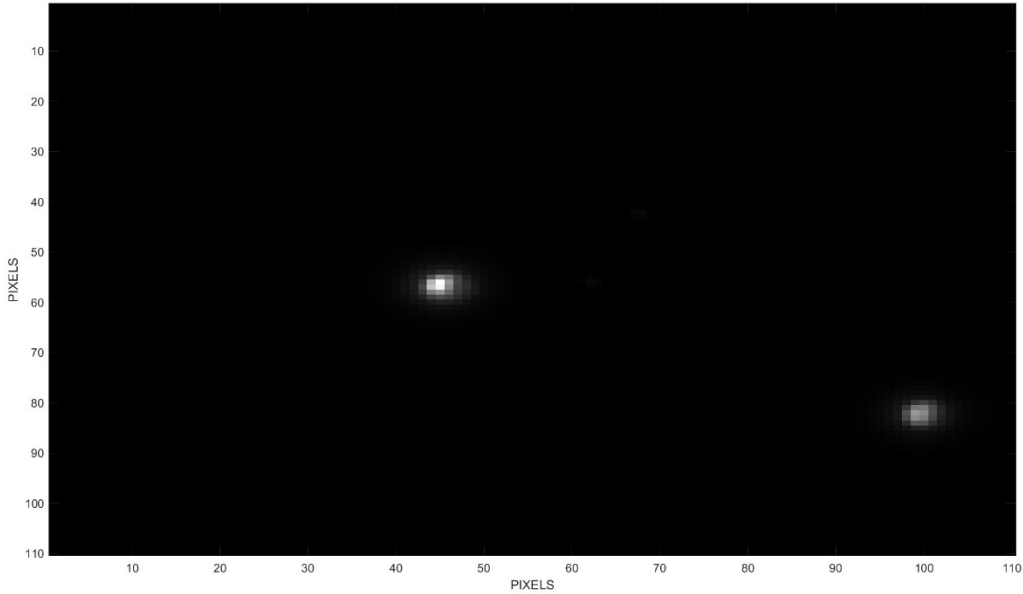


Figure 6: Image of the Earth/Moon system as seen by the proposed Earth/Moon tracker.

4. Simulation Results

One hundred frames of image data are simulated for each sensor to be compared in this study. The simulation methodology consists of randomizing the sampling phase of the CCD array with the image presented to it, by collecting the first sample at a random point in the 1 micro-radian sampled image produced by convolving the image shown in Figure 2 with the appropriate PSF/detector integration function. The actual location in angle space of the samples is stored so that this random phasing of the detector and image, doesn't produce a random line of sight variation (essentially the line-of-sight change is known). This random phasing will only measure how the sampling affects the ability of the centroid algorithm to reliably report the location of the object it is viewing.

It is assumed that the Earth and Moon are bright enough to be detected by the trackers. This is not a bad assumption since the average number of photons measured by the commercial sensor from the Earth is over 200 million photons and the Earth/Moon tracker measures well over 1 million photons per pixel. At these light levels the photon and readout noise tend to be fairly inconsequential to the noise caused by aliasing effects of the low resolution of the CCD detector compared to the maximum frequency passed by the optical system. The one hundred frames from both sensors are used to compute the centroid of the Earth location and the standard deviation of the location is reported in Table 3. Table 3 also reports the roll error estimated for the commercial star tracker as well as the roll standard deviation by taking the arctangent of the difference in the y-coordinates of the Earth and the Moon and dividing that by the difference in the x-coordinates.

Table 3: Sensor Performance in 3-axis while tracking the Earth/Moon

	Commercial Star Tracker	Earth/Moon Tracker
Pitch Deviation	8.9 μ Rad	0.26 μ Rad
Yaw Deviation	9.7 μ Rad	0.51 μ Rad
Roll Error/Deviation	12 mRad	6.7 mRad

5. Conclusions and Future Work

The new Earth/Moon tracking sensor delivers superior performance in spacecraft pointing simulations designed to test the effect of spatial aliasing online of sight variation. This simulation does not measure the effect of bias errors caused by albedo and phasing variations across the surface of the Earth. It does suggest that the new sensor design has the potential to aid in the pointing of laser communication beams to precise points on the Earth compared to the pointing that could be obtained from commercial star trackers. Sub-microradian pointing would allow for laser communication beams to be narrower, thus requiring less power compared to beams that would be designed to be larger to deal with the ambiguity in spacecraft pointing provided by existing star trackers.

Future work in this Earth/Moon tracker will focus on transmitting low resolution versions of images of the Earth obtained from geosynchronous weather satellites to the distant satellite to provide spatial corrections for Earth's albedo variation in the centroid measurements. These low-resolution images could be broadcast via radio communication channels since they would contain small amounts of data. This would allow the Earth/Moon tracker to remove bias errors in the estimate of the Earth's centroid. Other future work could involve laboratory measurements of the proposed tracking system using scale models of the Earth and Moon as viewed from Mars.

References

- [1] R. J. Wertz, *Spacecraft attitude determination and control*, Hingham MA: Reidel Publishing Company, 2012.
- [2] C. C. Liebe, "Accuracy Performance of Star Trackers-A Tutorial," *IEEE Transactions on Aerospace and Electronic Systems*, vol. 38, no. 2, pp. 587-599, 2002.
- [3] Deep Space Optical Communications, Hamid Hemmati, Jet Propulsion Laboratory, Pasadena CA, 2005
- [4] Richard D. Richmond and Stephen C. Cain, *Direct Detection LADAR Systems*, SPIE press, Bellingham, WA, 2010